EFFECT OF BOUNDARY CONDITIONS ON MICRODAMAGE INITIATION IN THIN PLY COMPOSITE LAMINATES

Luca Di Stasio[1,2,a], Janis Varna[2,b] and Zoubir Ayadi[1,c]

[1]Université de Lorraine, EEIGM, IJL, 6 Rue Bastien Lepage, F-54010 Nancy, France
[2]Luleå University of Technology, University Campus, SE-97187 Luleå, Sweden
[a]luca.di-stasio@univ-lorraine.fr, [b]janis.varna@ltu.se, [c]zoubir.ayadi@univ-lorraine.fr

Keywords: Polymer-matrix Composites (PMCs), Thin-ply, Transverse Failure, Debonding, Finite Element Analysis (FEA)

Abstract
The Energy Release Rate (ERR) and the contact zone size for a fiber/matrix interface debond are studied for a thin-ply glass fiber/epoxy laminate. The main objective is to analyze the effect on the debonding process of the presence of a traction free specimen surface or an adjacent material, in the form of a stiffer UD ply or by considering it as part of a thick 90° layer, at different levels of fiber content. To this end, a model of Representative Volume Element (RVE) subjected to different combinations of boundary conditions is proposed. It is found that the constraining effect of the adjacent ply favors at high fiber volume fractions the opening of small debonds ($10-40°$) for the same level of strain. The results agree well and provide a mechanical explanation to previous microscopic observations available in the literature [4].

1. Introduction

Thin ply composites represent today one of the most promising material for advanced applications in the aerospace industry and are attracting the interest of structural designers for use in mission-critical applications such as cryogenic tanks [1] and reusable space launchers' frames [2].

The experimental evidence on thin-ply laminates [3-6] confirms an earlier result on the influence of thickness and lay-up sequence on the strength and crack suppression behavior of FRP laminates, namely the existence of the so-called *thin-ply effect* and *in-situ strength*. At the end of 1970's, the experimental investigation of Bailey and collaborators [7,8] pointed out the relationship between ply thickness and transverse cracking, by showing that reducing the thickness of an inner 90°-ply in a cross-ply laminate results in the delay and even suppression of transverse crack propagation [9]. They identified the fiber-matrix property mismatch, and in particular the difference in Poisson's ratio, as the main mechanical driver of matrix cracks [10]. By investigating the micromechanics of transverse cracks, they observed that they originate as debonds or flaws at the fiber-matrix interface, which under increasing loads extend initially along the interface itself, then kink, coalesce and propagate as transverse cracks first through the thickness and finally through the width of the specimen [11].

Experimental evidence thus points to debonding at the fiber/matrix interface as the primary mechanism to investigate in order to achieve a better understanding about the initiation of transverse cracking and the potential of its suppression through an improved laminate design. It is paramount to this end to understand the process of fiber/matrix debonding, kinking and coalescence, as well as the

effect of ply thickness, non-uniformity of fiber distribution, material properties' mismatch and thermal strains. Cohesive zone modeling (CZM) has been one of the numerical strategies of choice to model these phenomena, often coupled with an elasto-plastic behavior for the polymeric matrix [12,13]. The method provides the possibility of simulating the onset and propagation of transverse cracks starting from a virgin ply, and can be used to record virtual crack path and loading histories which can then be compared with macroscopic experimental tests [14]. However, several drawbacks exist that cast a serious doubt about its applicability. First and foremost, the bi- and tri-axial stress state observed in inter-fiber regions and the cavitation-like matrix failure taking place at or close to the fiber interface [15-17] do not agree with the adhesive-like failure mechanism described by the CZM.

A second approach to the problem is the evaluation of the strain and stress state around the debond and consequent estimation of the Energy Release Rate (ERR) at the crack tip in mode I and mode II through the application of the Virtual Crack Closure Technique (VCCT) [18] and/or the J-integral method [19]. Its strength lies in the ability to provide direct comparisons of the magnitude of the effect on crack onset of different geometric, mechanical and thermal factors. However, unless coupled with a failure criterion as in [20], it has no predictive power regarding the direction of crack propagation and the size of the propagated crack. This approach was firstly used in the analytical treatment of the fiber/matrix interface problem in FRPC by Toya [21], and more recently in numerical analyses using the Boundary Element Method (BEM) [22] or the Finite Element Method (FEM) [23].

The recent advancements in thin-ply technology [2], where ply thickness can now be reduced to only 2-4 times the diameter of the reinforcement, has given a novel practical relevance to the theoretical analysis of advantages and disadvantages of using thin plies to delay intralaminar cracking. In this work we will compare the ERR related to the fiber/matrix debond growth for a debonded fiber placed in three different locations: a) at the free surface of the UD layer; b) at the interface with a very stiff layer of different orientation; c) as a repeating element in a thick layer. To magnify the expected trends, in cases a) and b) we analyze an extremely thin ply with only one fiber in the thickness direction. The effect of fiber content on fiber/matrix debonding is analyzed through the evaluation of Mode I and Mode II ERRs at the debond's crack tip using the Finite Element Method in conjunction with the VCCT and the J-integral method. Although extreme in its simplification, the model provides valuable insights of the constraining effect of adjacent plies and on the effect of fiber volume fraction, and thus on ply thickness.

2. The Model

In order to investigate the initiation mechanisms of transverse cracks, we focus our attention on the fiber/matrix interface and we apply the tools of Linear Elastic Fracture Mechanics (LEFM). We consider a 2-dimensional Finite Element (FE) model of a Representative Volume Element (RVE) consisting of a single row of glass fibers in epoxy matrix.

Several fibers have debonds of the same size at the interface with the matrix, indicated in red in Figures 1-4. An interaction between debonds is expected at high fiber content (especially between the closest ones), but the interaction will be the same for all the three analyzed cases of the top and bottom surfaces' constraints, which is the main subject for comparison in this paper. The selected configuration of debonds allows the selection of a Repeating Unit Cell (RUC) on which different surface constraints will be applied.

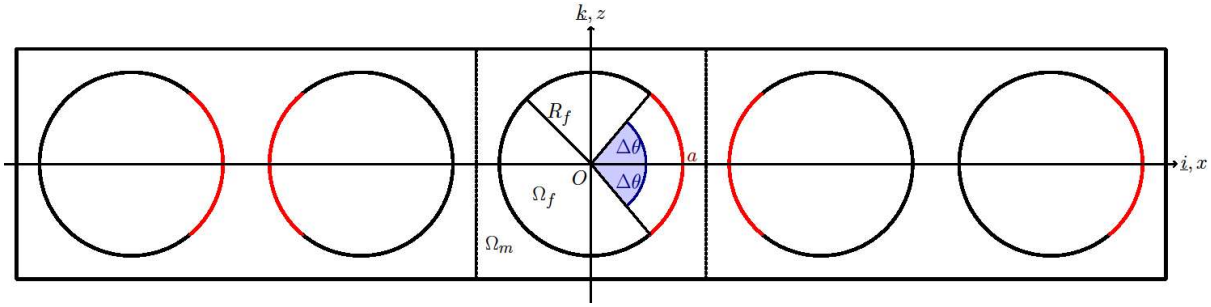

Figure 1. Schematic representation of a single "free" 90° ply with debonded fibers.

The first of such configurations, depicted in Figure 1, represents the case of a single ultra-thin ply with only one layer of fibers in the thickness direction. The bottom and top surfaces are traction-free: free surface in the FEM model (case *Free* in results). The second layup considered (Figure 2) corresponds to a single inner ultra-thin 90°-layer bounded by stiffer and thicker 0° plies, which is not bending and has a constant strain in the x-direction (the inhomogeneity and damage in the 90°-layer has no effect on strain in the 0°-layer). It is modeled by assigning a constant unknown vertical displacement to account for the Poisson's effect and a linear distribution of x-displacement on the top surface (case *Constant v, linear u* in results).

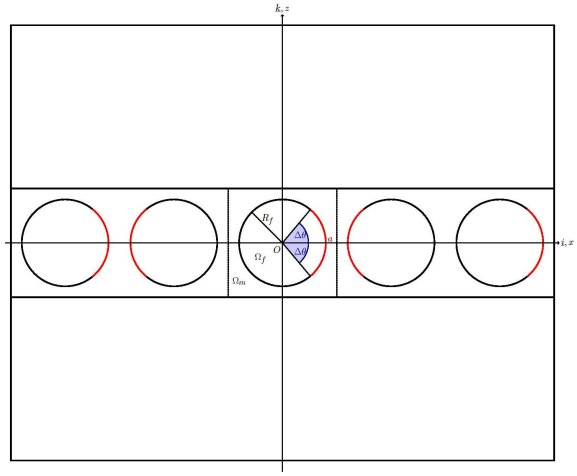

Figure 2. Schematic representation of the embedded 90° ply bounded by thick UD sections.

The final configuration, seen in Figure 3, represents a thick ply with fibers in square-packing arrangement in both the width and thickness direction. This last case is modeled by the application of a constant unknown vertical displacement on the top surface (case *Constant v* in results).

Pure plane strain conditions in the y-direction are considered and both the glass fiber and the epoxy are assumed to be isotropic materials with properties reported in Table 1.

Table 1. Material properties for glass fiber and epoxy.

Material	E [GPa]	ν[-]
Glass fiber	70.0	0.2
Epoxy	3.5	0.4

An arc crack is placed at the fiber/matrix interface, referred to as the *debond* in this article, where the matrix is debonded from the fiber (represented in Figure 4 in the deformed state). The debond is characterized by its angular size, equal to $2\Delta\theta$ and indicated in blue in Figure 4, and its position θ_0, taken as the angular position of debond's mid point. The debond's size is a free parameter, while its position θ_0 is in this paper assumed equal to 0, i.e. a centered debond symmetric with respect to the x-axis. At large sizes, the debond presents a so-called *contact zone* of angular size $\Delta\Phi$ close to the crack tip, where the crack faces are in contact and only Crack Sliding Displacement (CSD) is present. Only half of the RUC is considered and symmetry conditions are applied along the x-axis to model the presence of the lower half. Uniaxial tension is applied to the RUC in the form of an applied constant strain of 1% in the longitudinal direction.

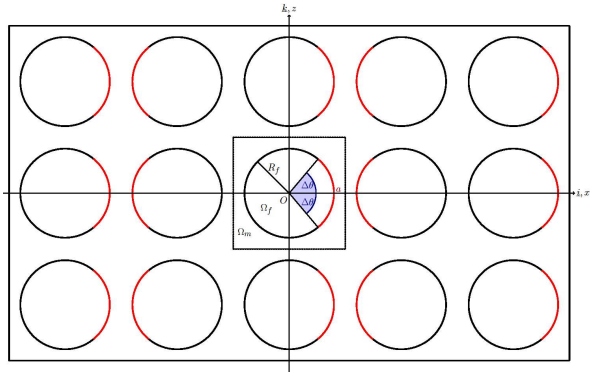

Figure 3. Schematic representation of the repeating element in the thick 90° ply.

The radius R_f of the fiber is assumed to be equal to 1 μm and the RUC's dimensions are $2L * L$, where the reference length L is governed by the fiber volume fraction V_f and the fiber radius R_f according to

$$L = \frac{1}{2} R_f \sqrt{\frac{\pi}{V_f}} \tag{1}$$

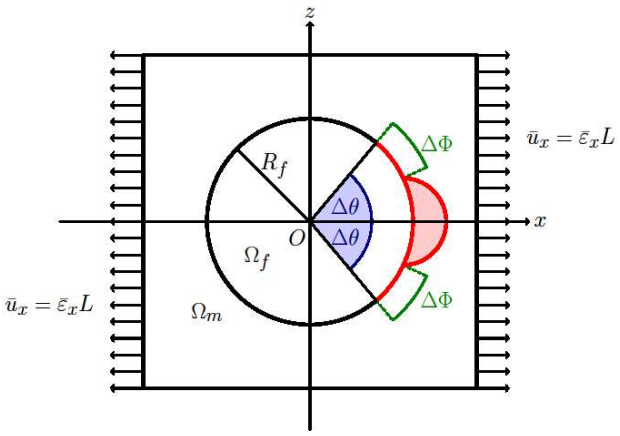

Figure 4. Schematic representation of the Representative Unit Cell (RUC) studied.

The FE model is implemented and solved using Abaqus Standard [54]. The Virtual Crack Closure Technique (VCCT) [42] is applied to the evaluation of the Mode I energy release rate (ERR), G_I, the Mode II ERR, G_{II}, and the total ERR, G_{TOT}. The total ERR is also calculated by means of the J-

integral method [43]. For the latter, the Abaqus built-in function is used; for the VCCT, an in-house Python routine has been developed. The model for a single fiber in an infinite matrix ($V_f = 0.0079\%$) is validated against the results obtained in [24] using the BEM in the case of a single fiber.

3. Results & Discussion

As seen in Figure 5, the Mode I Energy Release Rate shows a strong dependence on fiber content. The peak value at $V_f = 60\%$ is approximately 4 times the value at 20% and it is shifted towards lower debond's sizes. For $\Delta\theta > 60 - 70°$, Mode I ERR decays to zero signaling the emergence of the contact zone (see also Figure 7), where Crack Sliding Displacement (CSD) is the only component present.

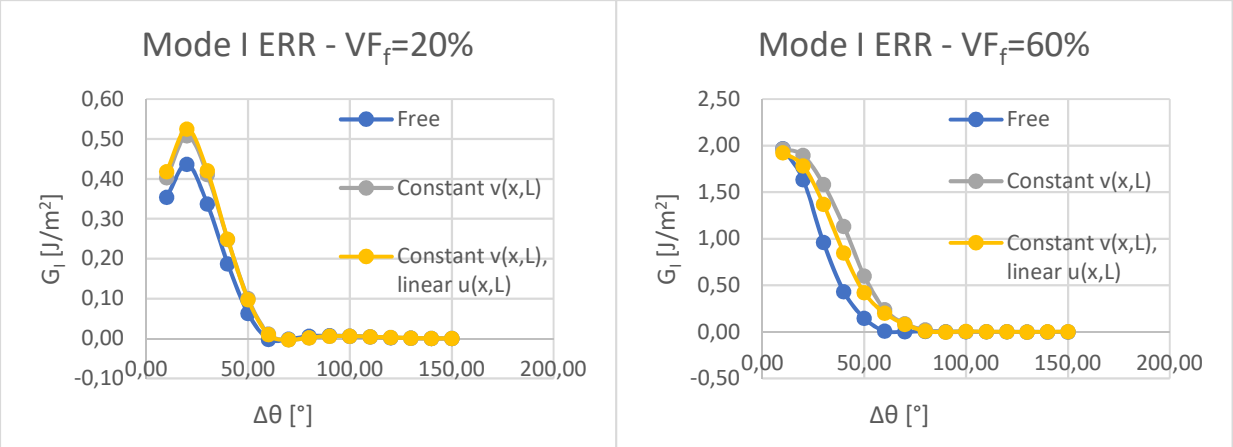

Figure 5. Evolution of G_I with respect to debond's size for the 3 models considered with 20% (left) and 60% (right) fiber content.

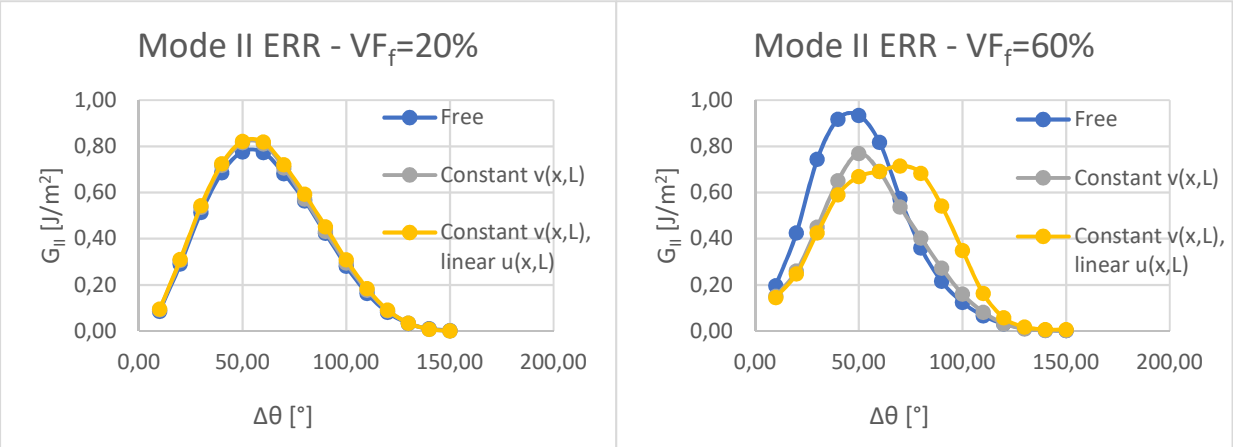

Figure 6. Evolution of G_{II} with respect to the debond's size for the 3 models considered with 20% (left) and 60% (right) fiber content.

The effect of boundary conditions is less pronounced, although present. In particular, the free surface case presents always lower values of G_I due to the ability of the matrix to comply locally, ability that

is prevented when the lateral movement of the surface is constrained by the adjacent material. This is an interesting result, because one would expect that closeness of the free specimen's surface would facilitate the debond growth. For the RUC (thick 90°-ply) at high fiber content, the value of G_I is higher as it reflects the presence of another identically debonded fiber on top of the analyzed (Figure 3), which interact with each other at higher V_f (i.e. lower RUC's thicknesses).

The mode II ERR (Figure 6) is on the other hand less sensitive to the change in fiber content, and thus on the presence of adjacent material. Changes in value do not exceed $15-20\%$ for any combination of fiber content and boundary conditions. As for mode I, increasing the fiber content enhances the effect of the adjacent material on crack initiation. When only the vertical displacement is constrained, mode II ERR is reduced by $15-20\%$; when the horizontal displacement is also imposed, a similar reduction in magnitude occurs but a longer plateau of maxima appears. The presence of a free surface favors Mode II, as it is shown by the approximately 20% increase in the value of G_{II} for a thinner ply.

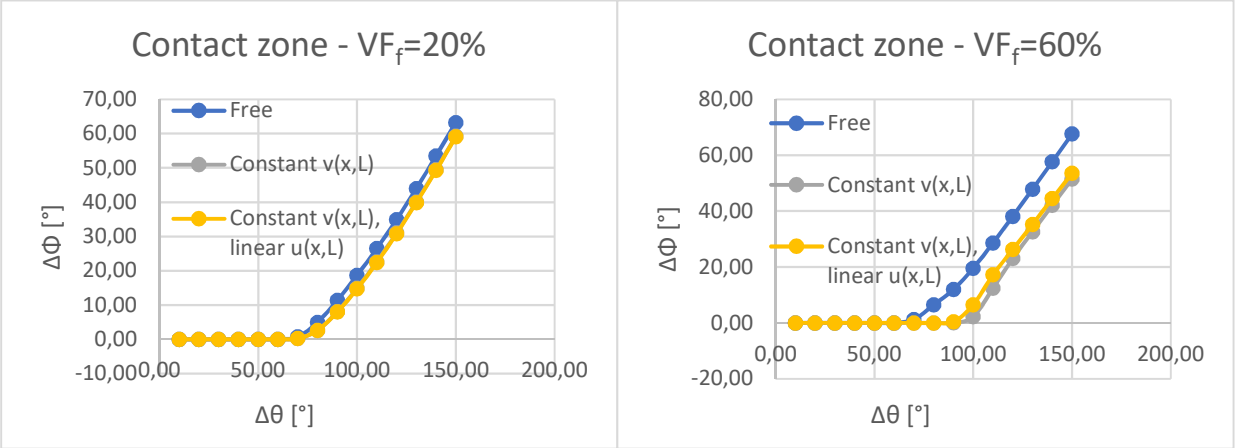

Figure 7. Evolution of contact zone size $\Delta\Phi$ with respect to debond's size for the 3 models considered with 20% (left) and 60% (right) fiber content.

The observed results can be explained in geometric and mechanical terms: under transverse tension, the matrix will contract toward the symmetry line more than the fiber due to the mismatch in Poisson's ratio. When the surface is free, for $\Delta\theta > 45$ the applied tension generates a radial Crack Opening Displacement (COD) equal to or smaller than the one created by the Poisson effect (opposite in sign, i.e. closing the crack), thus leaving the crack closed. The tangential components are instead coherent and sum up favoring a mode II crack initiation. When the vertical displacement is constrained, the COD component due to the Poisson's effect is reduced, thus favoring mode I at higher debond's size. The transition to a closed crack with a contact zone is thus delayed, but after the onset of the latter the behavior is unchanged. At larger debond's sizes, in fact, the main driver of crack sliding is the applied tension and not the Poisson effect, which induces displacements approximately normal to the interface and consequently does not have a relevant tangential component anymore. When an horizontal displacement is imposed to the RUC's surface however, it reduces at higher debond's sizes ($\Delta\theta > 60°$) the constraining effect of the bonded fiber/matrix interface in the near-tip region by forcing the matrix to follow the average applied tensile displacement. This, in turn, translates in a higher local tangential component of the crack faces displacement, which corresponds to higher values of G_{II} with respect to the other two combinations of boundary conditions. This favors mode II and creates the plateau seen in the picture on the right in Figure 6. The effect of fiber content is on the other hand explained by the de Saint Venant's principle: the lower the fiber content, the bigger the RUC and the less the debond is affected by perturbations in the elastic fields caused by the conditions at the boundary.

This mechanical explanation is confirmed by the evolution of the contact zone size (Figure 7). For low fiber content, the debond is not significantly affected by perturbations caused by boundary conditions and its evolution is thus independent from the latter. For high V_f, the constraing effect of adjacent material causes a delay of $30 - 40°$ in contact zone onset and a decrease in size of approximately 40°.

The numerical results presented agree and explain the microscopic observations of Saito & al. [4]. Working with $[0_2/90_n/0_2]$ laminate, with n = 1,2 and 4, they observed that thin plies favored the onset of debonds and their opening, which happened at strains lower than for thick plies. Coalescence of debonds and through-the-thickness propagation were instead delayed and even suppressed in the thinnest laminae.

4. Conclusions

The initiation mechanisms at the fiber/matrix interface in thin-ply laminates under transverse tensile strain have been investigated evaluating Mode I and Mode II ERRs and the contact zone's size. Three different cases have been considered: a) a debonded fiber close to the specimen free surface; b) a debonded fiber in the middle of a thick 90°-layer; c) a debonded fiber in the proximity of the interface with a stiff ply. These three configurations are modeled by different combinations of boundary conditions: case a) corresponds to a free surface in FEM model; in case b) a constant unknown vertical displacement is applied to upper surface; case c) is modeled by the concurrent application of a constant unknown vertical displacement and a linear horizontal displacement. Several values of fiber volume fraction have been evaluated, and the two extreme cases of $V_f = 20\%$ and $V_f = 60\%$ have been reported and analyzed to exemplify the trends found.

In accord with de Saint Venant's principle, it has been shown that the main consequence of ply thickness, controlled in the model by the fiber content, is to enhance the effect of the conditions applied to the boundary. This translates in a strong increase in the magnitude of mode I ERR, which is dominated by the applied uniaxial tensile displacement. The presence of a stiff material adjacent to a thin ply reduces mode II ERR, delays the onset of the contact zone and drastically reduces the size of the latter. The increase in mode I ERR with the concurrent decrease in mode II ERR and contact zone size for a constrained thin ply means that opening of the debond is favored for the same level of strain. This result agrees well and provides a mechanical explanation to the microscopic observations reported in [4], where it was noted that fiber/matrix debonds in thin plies appeared at lower strain levels than in thick plies.

Acknowledgments

Luca Di Stasio gratefully acknowledges the support of the European School of Materials (EUSMAT) through the DocMASE Doctoral Program and the European Commission through the Erasmus Mundus Program.

References

[1]J.R. Jackson, J. Vickers and J. Fikes. Composite Cryotank Technologies and Development 2.4 and 5.5M out of Autoclave Tank Test Results. *Composites and Advanced Materials Expo (CAMX), Dallas, TX, United States*, Oct. 26-29 2015.

[2]A. Kopp, S. Stappert, D. Mattsson, K. Olofsson, E. Marklund, G. Kurth, E. Mooij and E. Roorda. The Aurora Space Launcher Concept. *CEAS Space Journal*, 1-21, 2017.

[3]S. Sihn, R.Y. Kim, K. Kawabe and S.W. Tsai. Experimental studies of thin-ply laminated composites. *Composites Science and Technology*, 67(6):996-1008, 2007.

[4]H. Saito, H. Takeuchi and I. Kimpara. Experimental Evaluation of the Damage Growth Restraining in 90° Layer of Thin-ply CFRP Cross-ply Laminates. *Advanced Composite Materials* 21:57-66, 2012.
[5]A. Arteiro, G. Catalanotti, J. Xavier and P.P. Camanho. Notched response of non-crimp thin-ply laminates. *Composites Science and Technology*, 79:97-114, 2013.
[6]R. Amacher, J. Cugnoni, J. Botsis, L. Sorensen, W. Smith and C. Dransfeld. Thin ply composites: Experimental characterization and modeling of size-effects. *Composites Science and Technology*, 101:121-132, 2014.
[7]K. Garrett and J. Bailey. Multiple transverse fracture in 90 cross-ply laminates of a glass fibre-reinforced polyester. *Journal of Material Science*, 12(1):157-168, 1977.
[8]A. Parvizi and J. Bailey. On multiple transverse cracking in glass fibre epoxy cross-ply laminates. *Journal of Material Science*, 13(10):2131-2136, 1978.
[9]A. Parvizi, K.W. Garrett and J.E. Bailey. Constrained cracking in glass fibre-reinforced epoxy cross-ply laminates. *Journal of Materials Science*, 13(1):195-201, 1978.
[10]J. Bailey, P. Curtis and A. Parvizi. On the transverse cracking and longitudinal splitting behaviour of glass and carbon fibre reinforced epoxy cross ply laminates and the effect of Poisson and thermally generated strain. *Proceedings of the Royal Society of London A: Mathematical, Physical and Engineering Sciences: The Royal Society*, 599–623, 1979.
[11]J.E. Bailey and A. Parvizi. On fibre debonding effects and the mechanism of transverse-ply failure in cross-ply laminates of glass fibre/thermoset composites. *Journal of Material Science*, 16(3):649-659, 1981.
[12]V.I. Kushch, S.V. Shmegera, P. Brøndsted and L. Mishnaevsky Jr. Numerical simulation of progressive debonding in fiber reinforced composite under transverse loading. *International Journal of Engineering Science*, 49(1):17-29, 2011.
[13]M. Herraez, D. Mora, F. Naya, C.S. Lopes, C. Gonzalez and J. LLorca. Transverse cracking of cross-ply laminates: A computational micromechanics perspective. *Composites Science and Technology*, 110:196-204, 2015.
[14]L.P. Canal, C. Gonzalez, J. Segurado and J. LLorca. Intraply fracture of fiber-reinforced composites: Microscopic mechanisms and modeling. *Composites Science and Technology*, 72(11):1223-1232, 2012.
[15]L.E. Asp, L.A. Berglund and P. Gudmundson. Effects of a composite-like stress state on the fracture of epoxies. *Composites Science and Technology*, 53(1):27-37, 1995.
[16]L.E. Asp, L.A. Berglund and R. Talreja. A criterion for crack initiation in glassy polymers subjected to a composite-like stress state. *Composites Science and Technology*, 56(11):1291-1301, 1996.
[17]L.E. Asp, L.A. Berglund and R. Talreja. Prediction of matrix-initiated transverse failure in polymer composites. *Composites Science and Technology*, 56(9):1089-1097, 1996.
[18]R. Krueger. Virtual crack closure technique: History, approach, and applications. *Applied Mechanics Reviews*, 57:109-143, 2004.
[19]J.R. Rice. A Path Independent Integral and the Approximate Analysis of Strain Concentration by Notches and Cracks. Journal of Applied Mechanics, 35(2):379, 1968.
[20]V. Mantic. Interface crack onset at a circular cylindrical inclusion under a remote transverse tension. Application of a coupled stress and energy criterion. *International Journal of Solids and Structures*, 46(6):1287-1304, 2009.
[21]M. Toya. A crack along the interface of a circular inclusion embedded in an infinite solid. *Journal of the Mechanics and Physics of Solids*, 22(5):325-348, 1974.
[22]F. París, J. Cano and J. Varna. The fiber-matrix interface crack - a numerical analysis using boundary elements. *International Journal of Fracture*, 82(1):11-29, 1990.
[23]J. Varna, L. Zhuang, A. Pupurs and Z. Ayadi. Growth and interaction of debonds in local clusters of fibers in unidirectional composites during transverse loading. *Key Engineering Materials*, 734: 63-66, 2017.
[24]Abaqus V6.12. Analysis user's manual. Providence, RI, USA: Abaqus Inc.; 2012.